Volume 56
Number 63
14 August 2020
Pages 8871–9042

ChemComm

Chemical Communications

rsc.li/chemcomm

ISSN 1359-7345

ROYAL SOCIETY OF CHEMISTRY

FEATURE ARTICLE

Youhei Takeda, Przemyslaw Data *et al.*

Alchemy of donor–acceptor–donor multi-photofunctional organic materials: from construction of electron-deficient azaaromatics to exploration of functions

ChemComm

FEATURE ARTICLE

View Article Online
View Journal | View Issue

Cite this: *Chem. Commun.*, 2020, **56**, 8884

Alchemy of donor–acceptor–donor multi-photofunctional organic materials: from construction of electron-deficient azaaromatics to exploration of functions

Youhei Takeda, *[a] Przemyslaw Data *[bc] and Satoshi Minakata [a]

Received 8th May 2020,
Accepted 2nd July 2020

DOI: 10.1039/d0cc03322g

rsc.li/chemcomm

Electron-deficient azaaromatics play crucial roles in organic material fields. Therefore, the development of synthetic methods for electron-deficient azaaromatics and the exploration of their properties and functions is important for the advancement of materials sciences and related research fields. In this Feature Article, we describe new synthetic methods for exotic electron-deficient azaaromatics and their utilization in the design of multi-photofunctional organic materials. The key findings involve a novel oxidative skeletal rearrangement of binaphthaenediamines to give U-shaped azaaromics, *i.e.*, dibenzo[*a*,*j*]phenazine, in good yields. The unique physicochemical features of the dibenzophenazine allow for the development of multi-photofunctional organic materials based on a U-shaped and twisted electron-donor–acceptor-donor scaffold. The developed compounds exhibit efficient thermally activated delayed fluorescence, mechanochromic luminescence, and room-temperature phosphorescence, and they serve as emissive materials in organic light-emitting diodes.

[a] *Department of Applied Chemistry, Graduate School of Engineering, Osaka University, Yamadaoka 2-1, Suita, Osaka 565-0871, Japan. E-mail: takeda@chem.eng.osaka-u.ac.jp*
[b] *Faculty of Chemistry, Silesian University of Technology, M. Strzody 9, Gliwice 44-100, Poland. E-mail: przemyslaw.data@polsl.pl*
[c] *Center of Polymer and Carbon Materials, Polish Academy of Sciences, M. Curie-Sklodowskiej 34, Zabrze 41-819, Poland*

Introduction

Electron-deficient azaaromatics, such as pyridine-, pyrazine-, and pyridazine-fused compounds have attracted much attention in a wide range of research fields such as medicinal chemistry, catalysis science, and materials sciences. Focusing on the utility of electron-deficient azaaromatic compounds in materials

Youhei Takeda

Youhei Takeda received his PhD from Kyoto University under the supervision of Prof. Tamejiro Hiyama and Masaki Shimizu in 2010 and thereafter joined the Timothy M. Swager group at MIT as a post-doctoral fellow. He started his academic career as Assistant Professor at Osaka University in 2011, and he was promoted to Associate Professor in 2015. Concurrently, he was appointed as Adjunct Lecturer at Vietnam-Japan-University in 2015 and as Program Officer at the MEXT in 2019. His research interests include the design, synthesis, and interdisciplinary applications of hetero-atom-embedded exotic π-conjugated organic compounds.

Przemyslaw Data

Przemyslaw Data is currently working as Professor at the Silesian University of Technology, Poland. He received his PhD with honors in Chemistry (2013) at the Silesian University of Technology in Poland, and the work received Polish Prime Ministry Award for Outstanding Doctoral Dissertation. Straight after completing the PhD, Prof. Data received Mobility Plus funding followed by Marie Sklodowska-Curie Individual Fellowship to proceed with his scientific work at Durham University in the area of TADF emitters which resulted in MIT Innovator Under 35 award (2017 Polish Edition). His current research interest includes designing and analysis of organic small molecule and polymeric materials for organic electronics applications.

sciences, they serve as unique photo- and electro-active materials, as the replacement of C(sp^2)–H fragments of polyaromatic hydrocarbons (PAHs) with N(sp^2) units results in unique physicochemical properties (Fig. 1). For example, the N(sp^2) replacement for C–H enhances the electron affinities (EAs), leading to not only higher stability toward the air-oxidation but also more improved electron-accepting abilities when compared to their parent PAHs (Fig. 1a).[1] The embedment of electronegative N atoms into PAH main frameworks perturbs the electronic densities on the molecules and increases the dipole moments, thereby enhancing the solubilities into polar organic solvents (Fig. 1b) and manifesting specific stacking modes in the solid states (Fig. 1d).[2] Also, from the viewpoint of photophysics, the existence of lone pairs on the N atoms perpendicular to the π-electron systems plays a significantly important role in mixing energetically-close n–π* and π–π* excited states to yield large spin–orbit couplings (SOCs) (Fig. 1c).[3] Recently, this feature has been well considered to design organic emissive materials that utilize excited triplet states (T_n) such as thermally activated delayed fluorescence (TADF)[4] and room-temperature phosphorescence (RTP).[5] Another intriguing effect of the N(sp^2) substitution involves the manifestation of diverse molecular assembling modes in the solid states, due to the reduced numbers of C–H···π contacts when compared with their PAH analogues.[2] Many exotic packing modes, such as dimers and 1D-ribbons formed through complement N(sp^2)···H–C hydrogen bondings, and face-to-face slipped stackings of azaaromatics, have been reported (Fig. 1d).[2] Owing to the overviewed unique features, electron-deficient azaaromatics, specifically, linearly-fused azaacenes have been emerging as organic materials such as electron-transporting materials, n-type transistors, ion probes, organic memories, organic molecular conductors, and so on.[6] Also, the helicene-type azaaromatics have increasingly attracted much attention as chiroptical materials. Although there are several synthetic approaches to obtain such derivatives,[7] the optoelectronic applications of helical azaacenes have remained to be explored.[8]

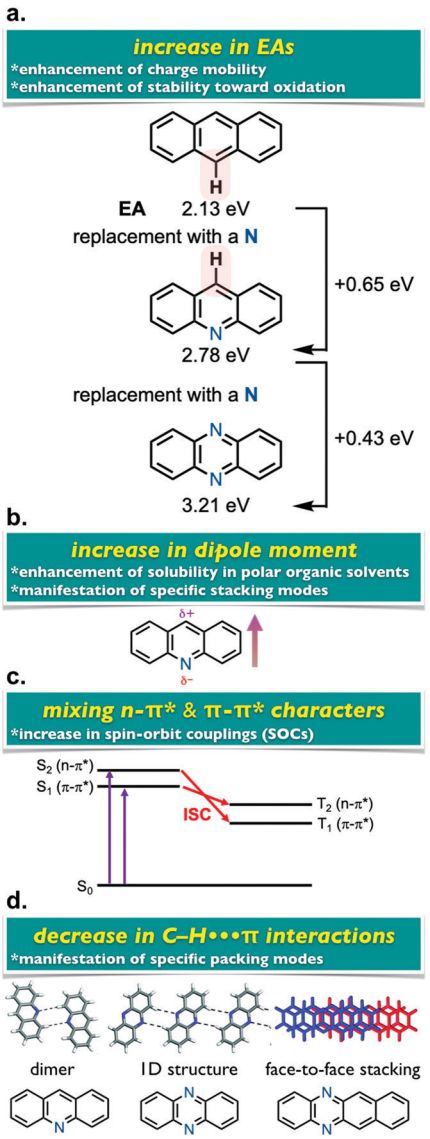

Fig. 1 Representative effects of the N(sp^2) replacement for C(sp^2)–H of PAHs. Adapted from ref. 2. Copyright 2011 American Chemical Society.

Satoshi Minakata

Satoshi Minakata received his PhD in 1993 from Osaka University under the direction of Prof. Yoshiki Ohshiro. After spending two years at DIC Corporation, he was appointed as Assistant Professor in Prof. Mitsuo Komatsu's group at Osaka University, and promoted to Lecturer in 2000. From 1997 to 1998, he worked with Prof. Erick. M. Carreira at California Institute of Technology as Visiting Associate. In 2002, he was promoted to Associate Professor and since 2010, he has been a Full Professor at Osaka University. His research interest centers the development of new synthetic methodologies for valuable organic molecules from simple molecules.

Given the functions of aromatic compounds highly depend on molecular structures, the development of new synthetic methods that allow for the access to exotic azaaromatic skeletons would provide us with tremendous opportunities to explore and discover new horizons of azaaromatic-based organic functional materials. Intuitionally, the oxidative fusion and annulation of aromatic amines would be a straightforward strategy for the construction of azaaromatic molecular architectures.[9] In fact, the serendipitous discovery of Mauveine by Sir William Perkin in 1896 testifies the high potential of direct oxidative annulation/fusion of aromatic amines.[10] However, as evident from the fact that Mauveine is an admixture of several constitutional isomers of phenazinium salts, the regulation of the oxidation of aromatic amines to provide structurally-well-defined azaaromatic products is a challenge in organic synthesis and organic materials sciences. In this Feature Article, (i) recent advancements of synthetic methods for exotic electron-deficient azaaromatic compounds through novel

oxidative transformations of aromatic diamines and (ii) the developments of multi-photofunctional organic materials[11] based on a donor–acceptor–donor (D–A–D) scaffold using an electron-deficient azaaromatic as the key electron-accepting core, mainly based on our contributions to the fields, have been overviewed.

Development of synthetic methods for electron-deficient azaaromatic compounds through novel oxidative transformations of aromatic diamines

In 2014, Takeda *et al.* serendipitously discovered a novel oxidative skeletal rearrangement of 1,1′-binaphthalene-2,2′-diamines (BINAMs) under the effect of 1,3-diiodo-5,5-dimethylhydantoin (DIH) to give a variety of dibenzo[*a*,*j*]phenazines (DBPHZs) (Fig. 2a).[12] Most importantly, the rearrangement involves the formal cleavage of the strong biaryl C–C single bond (the bond dissociation energy: *ca.* 118 kcal mol^{-1}) and the migration of a nitrogen atom onto the adjacent position (Fig. 2a). The developed reaction allows for the preparation of a variety of functionalized DBPHZs in good yields. It is noted that the dibrominated DBPHZs obtained by the rearrangement serve as useful synthetic building blocks for multi-photofunctional organic materials *via* Pd catalysis (*vide infra*). Mechanistic studies suggested the involvement of dearomatization process through the rearrangement, as naphthalene or a larger π-extended aromatic unit is required for the rearrangement to occur. The same research group investigated the unexplored physicochemical properties of DBPHZs and revealed that the DBPHZs are emissive in both solutions and solid states under the irradiation of UV light (Fig. 2b). Cyclic voltammetry of the DBPHZs in dichloromethane also revealed their high electron-accepting abilities and high EAs (3.12–3.34 eV),[12] which are comparable with that of well-known electron-transporting material, Alq_3.[13]

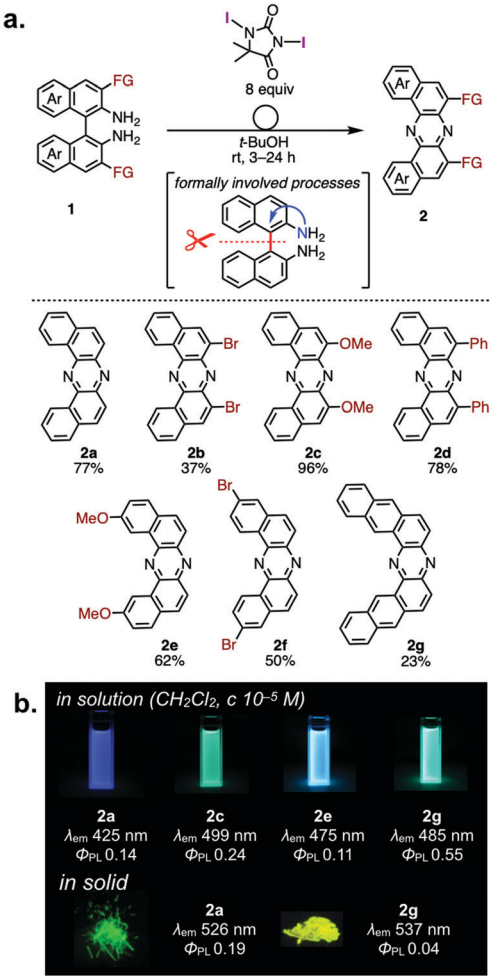

Fig. 2 (a) Oxidative skeletal rearrangement of BINAMs and (b) Photographs of solutions and solids of DBPHZs under UV lamp irradiation (λ_{ex} 365 nm). Adapted from ref. 12. Copyright 2014 The Royal Society of Chemistry.

During the investigation of the oxidative rearrangement, Takeda *et al.* also discovered the temperature- and halogenating reagents-dependent fates of the oxidation of BINAMs.[14,15] The treatment of BINAM **1a** with DIH at a low temperature (–40 °C) exclusively caused a distinctly different rearrangement to give spiro-type amidine **3a** in good yield (eqn (1)).[14]

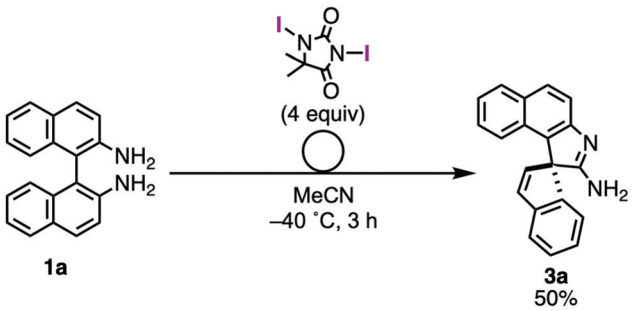

(1)

The amidine obtained by the rearrangement has a perpendicular π-scaffold and a functionalizable primary amino group. By taking advantage of such features, the same research group derivatized amidine **3a** into an N,O-coordinated 6-membered boron heterocyclic compound **5a** in 2 steps (Fig. 3a). The heterocycle **5a** displayed distinct aggregation-induced enhanced emission (AIEE)[16] (Φ_{PL} 0.13 in the solid states *vs.* Φ_{PL} < 0.01 in solutions), probably due to the rigid and perpendicular framework that prevents from dissipating excited energies through π–π interactions (Fig. 3b–d). A similar approach of the intramolecular N → B coordination to develop heterocyclic functional materials was reported by Min *et al.*,[17] where they utilize a linear azaacene derivative, resulting in a high EA (4.58 eV) and an extremely high electron mobility (1.60 cm^2 V^{-1} s^{-1}) in an n-type organic field-effect transistor (OFET) device. Taking into consideration that it is possible to tailor both emissive and mobility properties of an acceptor molecule, the post-functionalization of azaacenes through the intramolecular N → B coordination would find more applications in such as organic light-emitting transistors in the future.

In the oxidation of BINAMs, the switching of the electrophilic halogenating reagent from an I$^+$ equivalent (DIH) to a Cl$^+$ equivalent (*t*-BuOCl) in the presence of a base (2,6-lutidine) at

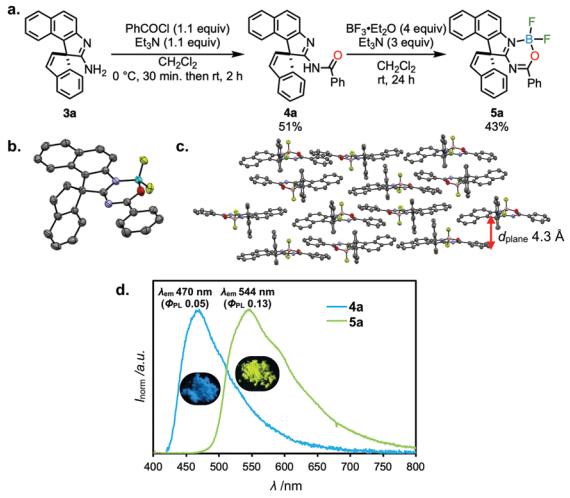

Fig. 3 (a) Derivatization of **3a** into AIEE-active spiro compound **5a**, (b) the molecular structure and (c) packing structure of **5a** in the crystal determined by the X-ray crystallographic analysis, and (d) emission spectra of **4a** and **5a** in solid states. Adapted from ref. 14. Copyright 2016 The Japan Institute of Heterocyclic Chemistry.

room temperature caused the oxidative ring-closure of BINAMs **1**, affording a variety of functionalized 7,8-diaza[5]helicenes **6** (Scheme 1).[15] All the diazahelicenes **6** are almost not emissive in solutions and solid states, probably due to efficient intersystem crossing (ISC) to the dark excited triplet states. However, the presence of functionalizable points in such as **6c** and **6d** would imply the possibility of tailoring photophysical properties by utilizing these compounds as building blocks for further chiroptical organic materials.

Another intriguing oxidative transformation of aromatic diamines to construct azaaromatics involves the oxidative self-annulation of 2,5-diaryl-3,4-diaminothiophenes **7** through the formal cleavage of a C–C and a C–S bonds, which was reported in 2017 by Takeda *et al.* (Scheme 2).[18] This reaction allows

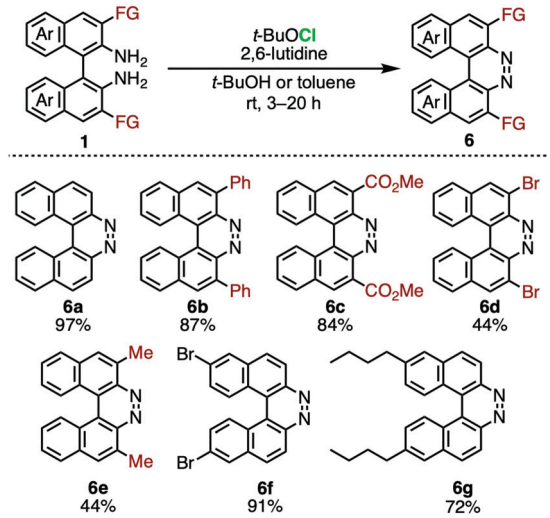

Scheme 1 Oxidative ring-closure of BINAMs to synthesize functionalized 7,8-diaza[5]helicenes.

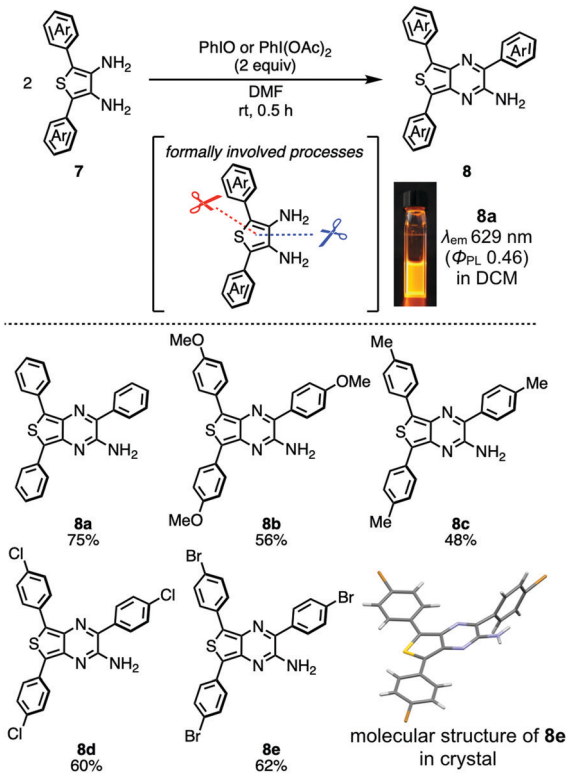

Scheme 2 Oxidative self-annulation of diaminothiophenes **7** to give aminothienopyrazines **8**.

preparing triaryl aminothienopyrazines **8**, which are otherwise difficult to synthesize by other existing synthetic methods. Since the thienopyrazine unit serves as a good electron-acceptor, the aminothienopyrazines are regarded as push–pull or donor–acceptor (D–A) π-conjugated systems. Due to the D–A electronic structure, a diluted dichloromethane solution of **8a** displays a typical intramolecular charge transfer (ICT) absorption (λ_{abs} 460 nm) and orange photoluminescence (λ_{em} 629 nm, the inset photograph in Scheme 2) with a good Φ_{PL} (0.46), showing a large Stokes shift (5840 cm^{-1}) typical to CT-emissive compounds. Also, it should be noted that aminothienopyrazine decorated with poly-halogens at the terminal aromatic rings (**8d** and **8e**) are available by the method (Scheme 2), which would serve as a monomer for branch-type emissive polymeric materials.

DBPHZ-cored D–A–D triads as multi-photofunctional organic materials

Thermally activated delayed fluorescent (TADF) materials

Purely organic thermally activated delayed fluorescence (TADF) materials have attached much attention in the field of organic electronics, as they can principally harvest 100% of triplet excitons in organic devices and convert into the light and thereby achieve much higher external quantum efficiencies (EQEs) of organic light-emitting devices (OLEDs) than those with a 1st generation fluorescent emitters.[4] A widely accepted molecular design for efficient TADF emitters involves D_n–A_m

(D = donor; A = acceptor; n, m = 1, 2, 3...) type π-conjugated compounds with large twist angels between the D and A moieties around the connecting bonds to minimize the energy gap (ΔE_{ST}) between the single excited state (S_1) and the triplet excited state (T_1). A very small ΔE_{ST} (<0.3 eV) is required for maximizing the reverse intersystem crossing (rISC) from T_1 to S_1 by thermal energy to yield TADF. In addition to the small ΔE_{ST}, the design strategy for enhancing SOC for the spin-forbidden S_1–T_1 transition is necessary. To do so, the incorporation of lone pairs can often contribute to the increase in a SOC by mixing n–π* and π–π* characters. What is also important is that the transition from a triplet state to a singlet state is allowed when these states have different characters (*e.g.*, n–π* to π–π* and *vice versa*).[19] The excited states of an organic D–A π-conjugated molecule are classified mainly into two types: locally excited (LE) states, *i.e.*, the ππ* excited states localized on the mutually perpendicular subsystems (D* or A*); intramolecular charge-transfer (CT) excited states, *i.e.*, the charge-separated excited states as a consequence of electron-transfer process from the D to A units [($D^{\bullet+}$–$A^{\bullet-}$)*].[20] According to the El-Sayed rule,[19] the transitions between ^{1}CT and ^{3}LE excited states (and *vice versa*) are allowed. A merit of using D–A molecule as a TADF material includes that the energy level of ^{1}CT excited state is finely tailored by tuning the electron-donating and electron-accepting ability of D and A units, respectively, and by fluctuating the D–A dihedral angles. Also, the CT state is highly affected by environmental conditions such as permittivity and viscosity. Since the LE states are less affected by these factors than CT states, the ΔE_{ST} and SOC are engineered by molecular design in a twisted D–A molecular scaffold. As a single molecule, one can usually distinguish between LE and CT excited states by spectroscopic techniques. Both of them can be observed as triplet or singlet. Nevertheless, to manifest CT excited state, there must be a difference in electric potentials between the two parts of the molecule. For this purpose, researchers are typically using N–C connecting bonds between electronic donors and acceptors. As already mentioned, DBPHZs serve as a luminogen with good electron-accepting abilities.[12] Considering those unique features, Takeda and Data designed DBPHZ-cored twisted donor–acceptor–donor (D–A–D) triads as TADF emitters for OLEDs.[21] An important value of DBPHZs in designing TADF materials includes that the triplet state of the DBPHZ-cored D–A–D molecules is localized on the acceptor (*vide infra*), which allows efficient rISC to ^{1}CT. Together with the tailoring of proper donors, the control of the emissive behaviour is implemented. In contrast to the mainstream of developing blue TADF materials at that time, the research team targeted the unexplored orange TADF materials:[22] the design of emissive organic compounds in the low-energies region (*i.e.*, orange, red, and near IR) is generally difficult by the conventional strategy of extending effective π-conjugation length, due to the energy gap low and the tendency of aggregation-caused quenching (ACQ) in the solid states.[23]

Dibrominated DBPHZ **2f** serves as an excellent electrophile in the Pd-catalyzed Buchwald–Hartwig double amination with a variety of diarylamine donors to afford U-shaped twisted D–A–D π-conjugated compounds **9** in good to excellent yields (Scheme 3).

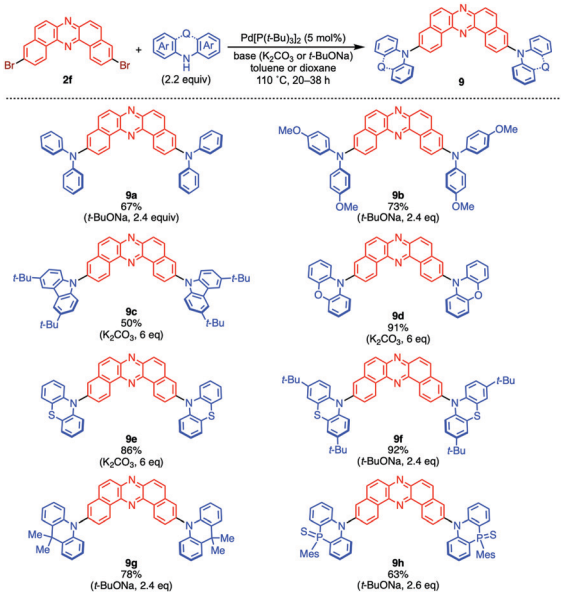

Scheme 3 Syntheses of D–A–D triads **9** through the Pd-catalyzed Buchwald–Hartwig double amination of **2f**.

The photophysical properties of the D–A–D triads are diversely tailored through the modification of D–A twisting angles and electron-donating abilities of the Ds. For example, a D–A–D compound having moderate D–A twist angles (*ca.* 50°) **9a** nicely displays positive solvatoluminochromism (*i.e.*, a phenomenon that the location of luminescence spectrum of a compound depends on solvent polarity) as the function of solvent polarity (Fig. 4), due to the ICT character in the excited states (^{1}CT).[24] This sensitivity of emission color toward slight change in dielectric constants would be useful for designing probes for visualizing environment conditions such as polarity and viscosity.[25]

The D–A twisting angles significantly affect the ΔE_{ST} (Fig. 5), and an almost perpendicular D–A angle (in the case of **9d**) allows a very small ΔE_{ST} value (80 meV), due to the decoupling of the electronic interactions between the Ds and A core.[21] Another specific feature of the series of twisted D–A–D compounds is the 1st triplet excited state (T_1) is localized on the acceptor (DBPHZ) unit (^{3}LE$_A$), which is evident from the similar

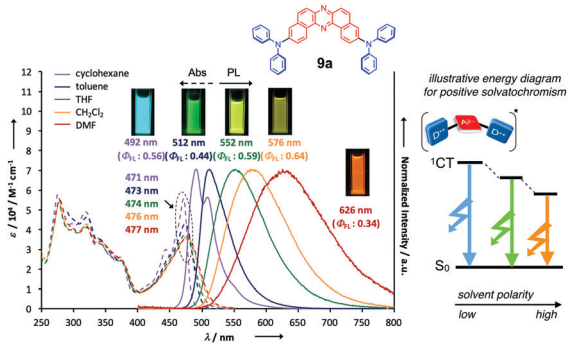

Fig. 4 UV-vis and PL spectra of **9a** in various organic solvents. Adapted from ref. 24. Copyright 2017 The Royal Society of Chemistry.

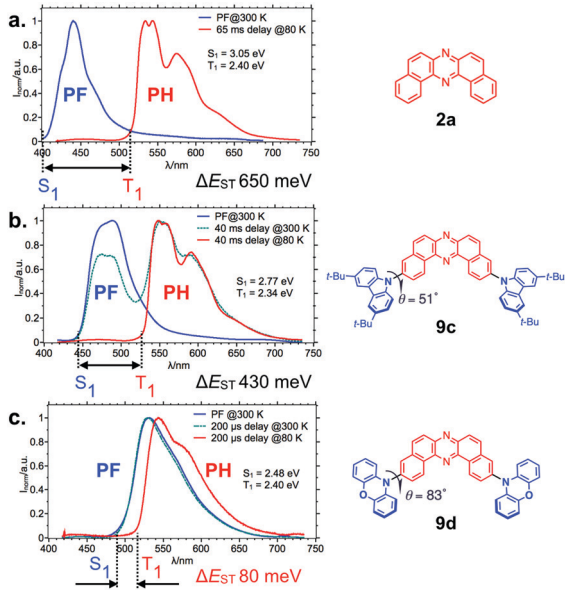

Fig. 5 Prompt fluorescence (PF, blue lines) and phosphorescence (PH, red lines) spectra of (a) **2a**, (b) **9c**, and (c) **9d** in Zeonex® matrix. The D–A twist angles are estimated by the DFT method at the B3LYP/6-31+G(d,p) level.

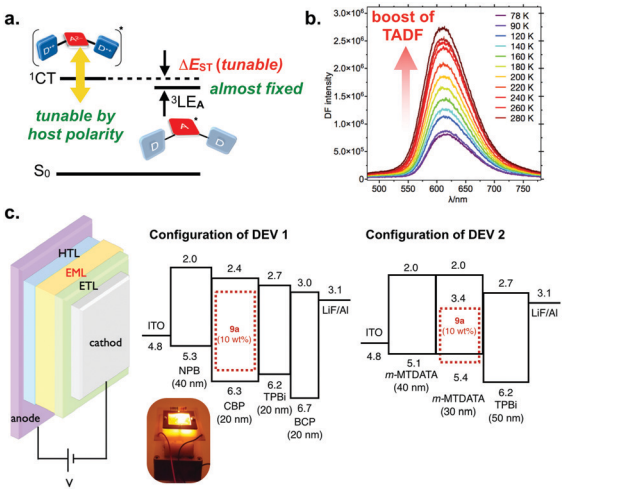

Fig. 6 (a) A schematic illustration of energy diagrams of D–A–D compounds **9**, (b) temperature-dependency of the PL spectra of **9d** in CBP host, and (c) configurations of OLED devices fabricated with **9d**. The inset photograph shows the OLED device (DEV 1). Adapted from ref. 21. Copyright 2016 Wiley-VCH Verlag GmbH.

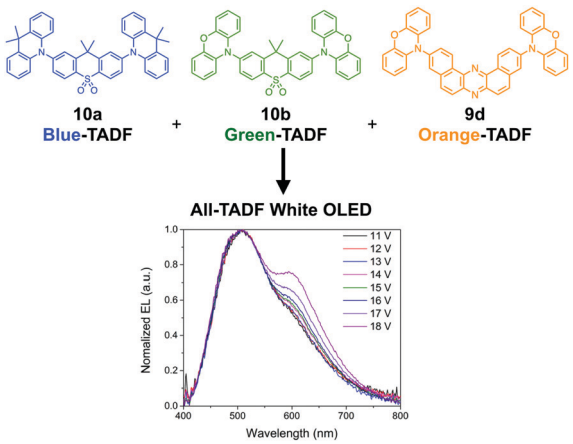

Fig. 7 All-TADF white-OLEDs. Adapted from ref. 26. Copyright 2017 Springer Nature.

phosphorescence spectra of the D–A–D compounds (red lines in Fig. 5b and c) with that of the acceptor material in Zeonex® matrix (red line in Fig. 5a).[18] Zeonex® is a non-polar cycloolefin polymer and featured with high transparency in UV-vis region. These features are suitable for the investigation of intrinsic photophysical properties of an emissive compound in a dispersed state, by minimizing the electronic interactions between an emissive compound and polymer that can affect the photophysical properties of the entire composite film.

By making the use of the almost fixed value of ^3LE_A energy (*ca.* 2.40 eV) and the variable nature of environmental polarity-depending ^1CT energy, the ΔE_{ST} value is further engineered by selecting host materials with appropriate polarity (Fig. 6a). In fact, the ΔE_{ST} of **9d** is further diminished to as narrow as 20 meV in a more polar host CBP [4,4′-bis(*N*-carbazolyl)-1,1′-biphenyl], and the rISC is significantly boosted to yield orange TADF as a function of the rise of temperature (Fig. 6b). In addition to efficient TADF behaviour in host matrix, D–A–D compound **9d** shows beautiful reversible electrochemical redox properties (IP/EA 5.36/3.38 eV) and high thermal stability (T_d (5 wt%) 453 °C). Owing to these features, the triad **9d** serves as an efficient TADF emitter in OLED device (DEV 1 in Fig. 5c), and the OLED device fabricated with **9d** achieved a high maximum EQE up to 16%, which is much higher than the theoretical maximum EQE of OLEDs using a 1st generation fluorescent emitter (*ca.* 5%). The authors also discovered an intriguing effect of host material on the emission outcomes: an unusual NIR EL emission (λ_{em} 741 nm) from the OLED fabricated with emitter **9d** and *m*-MTDATA (DEV 2 in Fig. 5c) is realized with a high EQE (*ca.* 5%) for NIR-emissive OLEDs.[21]

By making the use of broad Gaussian-type CT emission spectra of D–A–D emitter **9d**, de Sa Pereira *et al.* realized white-emitting OLEDs comprising of all-TADF-emitters (Fig. 7).[26]

The systematic investigations of the configuration of OLEDs and composition of blue, green, and orange TADF emitters led to the optimal structures of OLED devices. Combining with the blue (**10a**), green (**10b**), and orange (**9d**) TADF emitters, the maximum EQE reached a high value (*ca.* 16%) with a low-efficiency roll-off (11% at 1000 cd m^{-2}).

Nowadays, many different D–A–D type emitters that include our acceptor are studied. For example, recently, D_n–A dibenzo[*a*,*c*]phenazine derivatives have been developed as TADF emitters for the OLEDs application by Sun *et al.*,[27] although the efficiency does not exceed 12%.[27] Also, the DBPHZ is used as a core for TADF emitters patented as materials for smartphones screens.[28] These examples clearly show that the donors-installed phenazine-fused azaaromatics is a promising scaffold for optoelectronic materials. Nevertheless, they are all assumed to be "mono-functional" organic materials such as simple OLED emitters.

This would make scientists think more about the functions, raising questions such as "what else could be done with the D–A–D scaffold?", "should we limit to mono-functional materials?", and so on.

DBPHZ-cored D–A–D triads as beyond single photo-functionality

Many researchers working on luminescent materials would be wondering how many photofunctional aspects of an emissive compound they do see. In our opinion, the functions of materials would be like seeing faces of polyhedral of functions (Fig. 8). Some aspects are well-seen from the point we are standing at, while others might be hidden from our sight (Fig. 8). Thus, if we can deduce as many photofunctions as possible of the emitter beyond the single-use, potential new applications and new utilities of the emitter are expected.[9]

Mechanochromic luminescent (MCL) materials have attached much attention, due to the possible applications such as security inks, luminescence sensors, ratiometric bio-probes, and display materials.[29] In 2017, Takeda *et al.* showcased the realization of the first example of TADF-active multi-color-changing MCL materials based on the TADF-active DBPHZ-cored D–A–D scaffold.[24] To design MCL-active and TADF materials, the research team applied a simple but very effective trick of element-replacement strategy to regulate conformations of the D–A–D compound (Fig. 9). A TADF-emitting D–A–D compound **9d** can take almost the single conformation, where the almost planar phenoxazine (POZ) donors are perpendicularly oriented toward the DBPHZ acceptor (Fig. 9a). In contrast, a phenothiazine (PTZ) can take boat conformation (Fig. 9b), due to a larger atomic radius of the sulfur atom (0.88 Å) than that of the oxygen atom (0.48 Å).[30] As a consequence, a substituent on the nitrogen of PTZ can occupy the *quasi*-axial (ax) or equatorial (eq) positions, giving rise to two

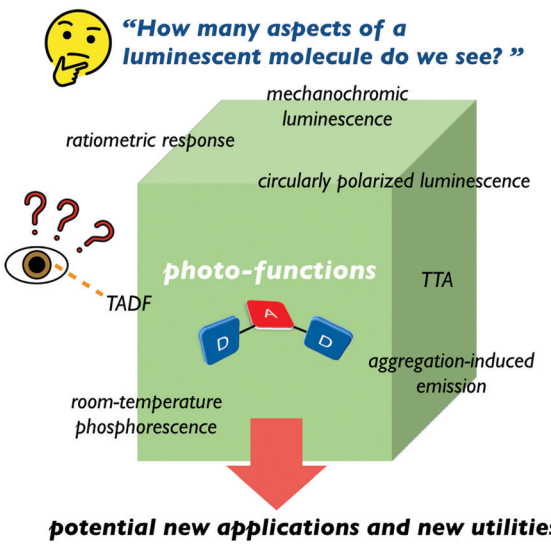

Fig. 8 Aspects of a luminophore. All emoji designed by OpenMoji-the open-source emoji and icon project. License: CC BY-SA 4.0.

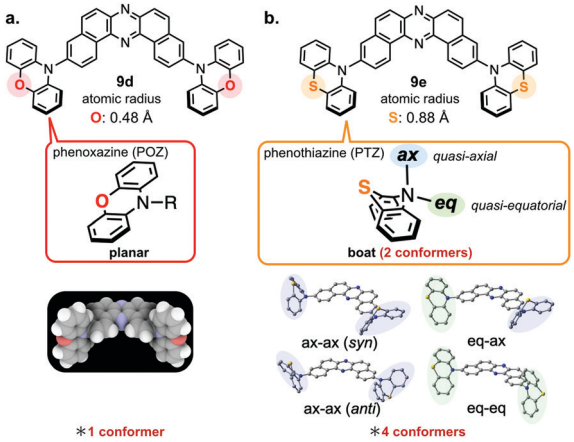

Fig. 9 Molecular design of MCL-active TADF material **9e**.

conformers (Fig. 9b). As the results, a D–A–D molecule **9e**, which has two PTZ units, can take 4 possible conformers (*syn*-ax–ax, *anti*-ax–ax, eq–ax, and eq–eq, Fig. 9b) with distinctly different electronic structures, leading to different emission colors.

Takeda and Data *et al.* nicely provided the proof-of-concept by investigating the photoluminescence profiles of the solids of **9e** upon the application of various external stimuli (Fig. 10).[24] The D–A–D compound **9e** displayed a significant change in appearance and photoluminescence colors in response to various external stimuli such as grinding, heating, and fuming (Fig. 10a). The importance of the sulfur atom for this multi-color-changing MCL is evident, as the D–A–D analogues with carbon-bridge (**9g**), without a bridge (**9a**), and oxygen-bridge compounds (**9d**) did not exhibit such drastic emission color change toward the external stimuli. The X-ray crystallographic analysis of a single crystal of **9e** grown from a dichloromethane solution clearly shows that the acceptor can take both ax and eq

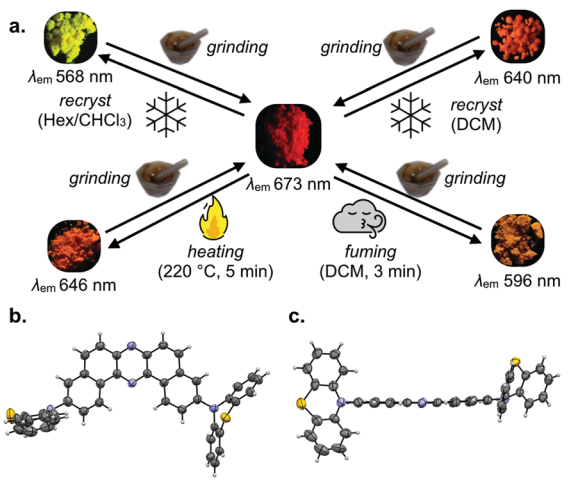

Fig. 10 (a) The emission color responsivity of the solids of **9e** toward the application of external stimuli. (b) The top view and (c) the side view of the molecular geometry of **9e** in the single crystal grown from its dichloromethane solution. Adapted from ref. 24. Copyright 2017 The Royal Society of Chemistry. All emoji designed by OpenMoji-the open-source emoji and icon project. License: CC BY-SA 4.0.

conformations of the donors (Fig. 10b and c). It should be noted that the D–A–D compound **9e** also displays an efficient orange TADF in a host matrix such as Zeonex®, which is evident by a very narrow ΔE_{ST} (80 meV) comparable with that of oxygen-analogue **9d**. Also, the OLEDs fabricated with **9e** in a more polar host CBP achieved as high maximum EQE as 17%, indicating that the TADF performance is maintained through the replacement of the bridging-oxygen atoms with sulfur atoms.

Given conventional approaches for designing MCL materials that can convert multiple meta-stable states utilize the difference in molecular assemblies (Fig. 11a),[29] the approach presented by Takeda *et al.* is a new promising one for realizing multi-color changing MCL materials that are mainly dictated by the conformational fluctuation (Fig. 11b).

The photophysics of solids **9e** that show different colors were investigated in detail by time-resolved spectroscopy by Data *et al.*[31] Importantly, it was revealed that not only emission colors but also photophysical dynamics are different in different conforms.[31] The research team also demonstrated that the solution processes using different polarity solvents can result in different EL colors by fluctuating dominant conformers through the fabrication process. Such unique tunability of the emissions by conformational fluctuation could allow the implementation of more and more solution-processed productions of OLED devices and security inks.

Takeda, Penfold, and Fukuhara recently investigated the effect of hydrostatic pressure on the photophysical properties of **9e** in solution, where the fluctuation of molecular conformations would be more sensitive toward the materials environments.[32] In contrast to the solid states, **9e** in toluene shows 3 distinct CT emissions derived from the 3 different conformers (eq–eq, ax–eq, and ax–ax types) (Fig. 12a). The application of hydrostatic pressure allows for the regulation of TADF by restricting the vibration and rotation of the donor units around the C–N connecting bonds to suppress spin-vibronic coupling, which represents the first example of regulating TADF emission by external pressure.

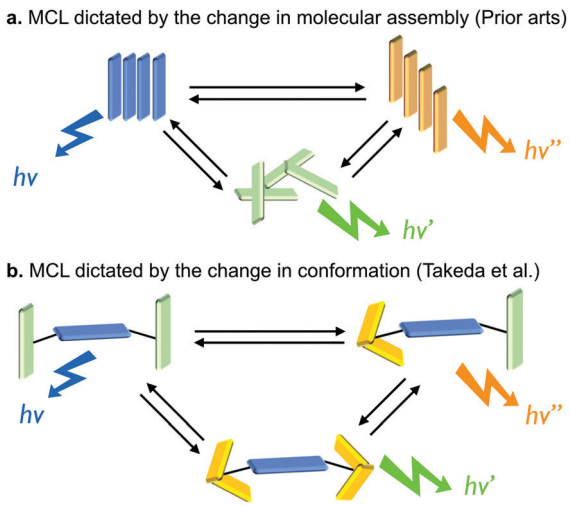

Fig. 11 Schematic representations for MCL dictated by (a) molecular assemblies and (b) molecular conformations.

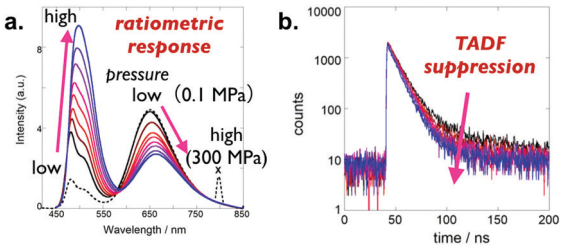

Fig. 12 Change in (a) photoluminescence spectra and (b) luminescence decay of a toluene solution of **9e** as a function of hydrostatic pressure. Adapted from ref. 32. Copyright 2019 Wiley-VCH Verlag GmbH.

The MCL material **9h** based on the conformational regulation was developed by Takeda and Data by introducing conformationally flappy but with less-electron-donating units (dihydrophenophosphanizine sulfide: DPPZS) (Fig. 13b).[33] As expected, the compound **9h** displays multi-color-changing MCL behaviour toward various stimuli such as grinding, heating, and vapor fuming (Fig. 13c). In addition, the MCL material also shows response toward the vapor of acid (trifluoroacetic acid: TFA) and base (triethylamine: TEA) to drastically change emission colors in a reversible way (Fig. 13d). The very large shift in emission colors between the visible and NIR region (5792 cm^{-1}) with a single molecule is rare and thus worth noting.

Single crystal-to-single crystal (SC-to-SC) transition of the crystal containing only eq–eq **9h** was caused by the evacuation of crystal solvent ($CHCl_3$), which led to a significant change in the orientation of a donor against the acceptor without a noticeable change in intermolecular distances (Fig. 14).[33] The SC-to-SC transition caused a large red-shift of the PL spectra (Fig. 14), which gives direct evidence of the conformational effect on emission properties.

Another important aspect of installing DPPZS donors into the A unit involves the manifestation of dual emission of TADF and room-temperature phosphorescence (RTP) from **9h** (Fig. 15a).[33]

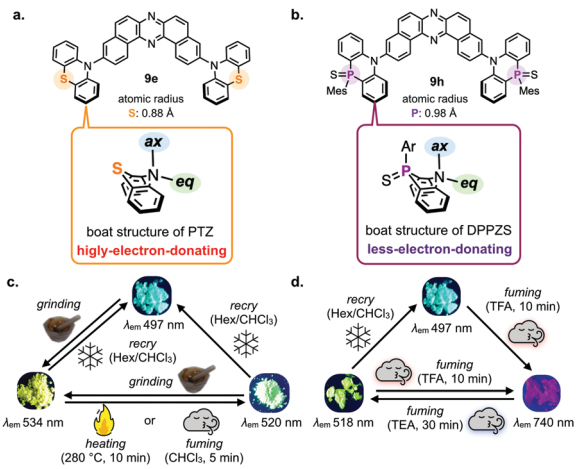

Fig. 13 Comparison of the design of (a) **9e** and (b) **9h**. Emission color responsivity of the solids of **9h** toward the application of (c) external stimuli and (d) acid/base vapor. Adapted from ref. 33. Copyright 2018 The Royal Society of Chemistry. All emoji designed by OpenMoji-the open-source emoji and icon project. License: CC BY-SA 4.0.

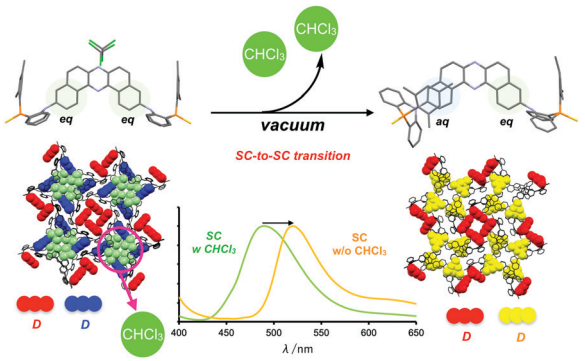

Fig. 14 Schematic illustration of SC-to-SC transition and PL spectra of before (green) and after (orange) the transition. Adapted from ref. 33. Copyright 2018 The Royal Society of Chemistry.

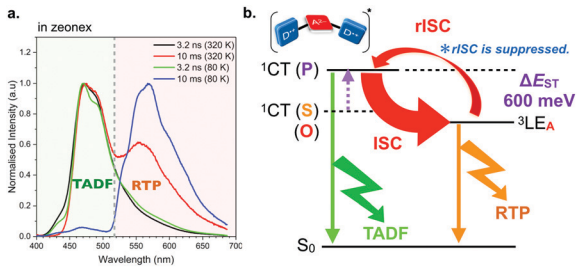

Fig. 15 (a) Time-resolved PL spectra of **9h** in Zeonex® and (b) a plausible mechanism for dual emission of TADF and RTP from **9h** in Zeonex®. Adapted from ref. 33. Copyright 2018 The Royal Society of Chemistry.

The authors propose that the destabilization of ^{1}CT excited state by lowering electron-donating ability of the D unit results in a moderate ΔE_{ST} (600 meV in Zeonex®) and thereby the rISC from the ^3LE_A excited state becomes sluggish and RTP is concomitantly observed (Fig. 15b). Such dual emission feature might be useful for developing single molecular white-emitting materials. Also, the result would provide opportunities for switching TADF and RTP by the engineering of ΔE_{ST} values by molecular design, which should be a new horizon of organic materials researches.

Very recently, the group led by Takeda *et al.* utilized the U-shaped structure of DBPHZ acceptor for constructing a new class of π-conjugated D–A–D–A macrocycle **10** (Fig. 16a).[34] The U-shaped structure was found suitable for synthesizing **10**, especially macrocyclization proceeds in a rather efficient manner. The authors proposed that the utilization of the propeller structure of triarylamine to regulate the conformation of the precursor for **10** to make the macrocyclization process efficiently. The macrocycle forms two polymorphs that have helical and saddle conformations (Fig. 16b and c), which distinctly show different emission colors (Helical: λ_{em} 594 nm; Saddle: λ_{em} 654 nm). Based on the theoretical calculations, the Saddle is the more thermodynamically stable conformer as the single molecule. Both conformers show beautifully-aligned and porous packing structures in the single crystals (Fig. 16b and c). Especially, the Saddle conformer forms complementary pairs through intermolecular D···A interactions, which results in highly aligned columns with molecular size cavity (9.7–10.2 Å, Fig. 16c).

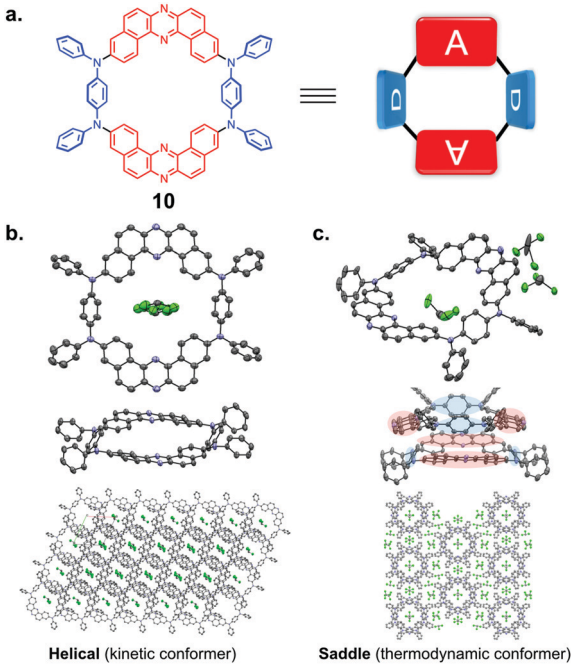

Fig. 16 (a) Chemical structure of **10**. Molecular geometries and packing structures in the single crystals of (b) helical and (c) saddle conformers, revealed by the X-ray crystallographic analyses. Adapted from ref. 34. Copyright 2020 American Chemical Society.

The authors also investigated the effect of macrocyclization of D–A–D–A scaffold on the physicochemical properties by comparing with a linear compound **11**, which is regarded as an open-form of macrocycle **10** (Fig. 17a). One of the impressive results here involves a much higher contribution of TADF in photoluminescence of macrocyclic compound **10** than linear

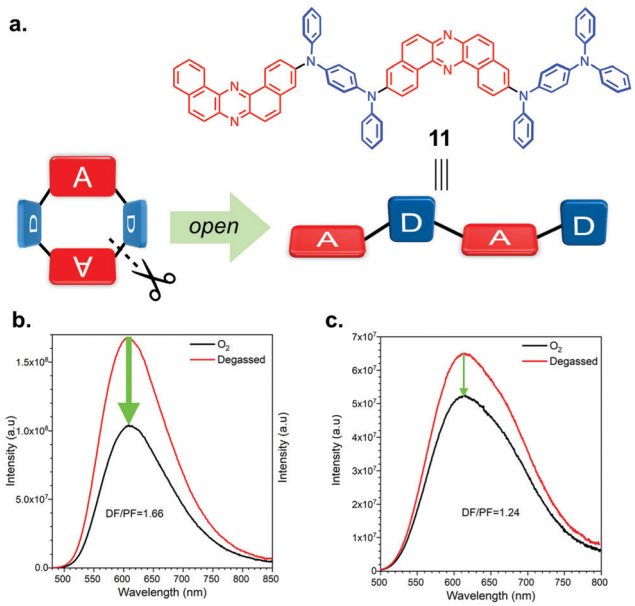

Fig. 17 (a) Chemical structure of **11**. Steady-stated PL spectra of (b) macrocycle **10** and (c) linear analogue **11** in toluene (5 μM). Adapted from ref. 34. Copyright 2020 American Chemical Society.

analogue **11**, which is evident by the sensitivity of the PL intensity toward the air (Fig. 17b and c). The linear compound has more conformational freedom arising from the rotation around the D–A connecting C–N bonds when compared to the macrocycle. Higher conformational flexibility and greater conformational inhomogeneity of **11** would contribute to more non-radiative pathways through molecular vibration and bond rotations. The similar trend for TADF efficiency is true for OLED devices: the OLEDs fabricated with macrocycle **10** achieved a relatively high EQE (11.6%), which is much higher than that with linear analogue **11** (6.9%) and the theoretical maximum of a 1st generation fluorescent emitter (*ca.* 5%). This work represents the first example of macrocyclic-TADF-OLEDs exhibiting a distinctly measurable EQEs. The results shown by the authors would open up new avenues toward developing macrocyclic TADF materials having value-added functions in optoelectronics and supramolecular sensors in the future.

Conclusions and perspectives

In summary, we have overviewed recently developed novel oxidative synthetic transformations of aromatic diamines into exotic structured electron-deficient azaaromatics. Also, the development of a series of twisted D–A–D compounds that display multi-photofunctionalities by making the use of good electron-accepting ability and luminescent character of the DBPHZ core, have been compiled. The investigation of a series of the D–A–D compounds led to the discovery of notable effects of bridging-heteroatoms of the diarylamine donors on their photophysical properties such as mechanochromism, thermally activated delayed fluorescence, and room-temperature phosphorescence. Furthermore, the unique U-shaped structure of DBPHZ provides an opportunity to make a new D–A–D–A type π-conjugated macrocycle, which clearly showed us the effect of macrocyclization of D–A fragment on the TADF properties. Also, the first macrocyclic TADF material-based OLEDs have been assessed. We believe that this Feature Article showcases how powerful the synergy of the reaction development and spectroscopy-based materials investigations is. As for the perspective, we would like to answer the previous question ''should we limit to monofunctional materials?''. The simplest answer supported by our presented finding is ''no'': organic compounds give so many possibilities of tailoring molecules' properties that we should use all the opportunities to effectively use our materials. As for the organic core, further exploration of exotic organic materials based on the DBPHZ core and other azaaromatics would provide great opportunities for discovering new materials that deserve the future applications in optoelectronics and sensors. But, once again, we should not limit our ideas to the above-mentioned ones: it is difficult to expect what the future and new molecules and applications will bring. The closest applications include organic light-emitting transistors and sensor OLEDs, where by changing local pressure, temperature and/or air contaminations, the emission color quickly and drastically changes. In the era, where smartphones are everywhere and everything tries to be smart, wearable electronics will become more and more indispensable for our life and will be implemented in our clothes and bodies. For such applications, the ''flexible'' solutions and electronics are necessary, and definitely, the MCL materials will find their place there.

Conflicts of interest

There are no conflicts to declare.

Acknowledgements

This work was supported by a Grant-in-Aid for Scientific Research on Innovative Areas ''π-System Figuration: Control of Electron and Structural Dynamism for Innovative Functions'' (JSPS KAKENHI Grant Number JP17H05155, to YT), ''Aquatic Functional Materials: Creation of New Materials Science for Environment-Friendly and Active Functions'' from the MEXT (JSPS KAKENHI Grant Number JP19H05716, to YT), by a Grant-in-Aid for Scientific Research(B) (JSPS KAKENHI Grant Number JP20H02813, to YT), and by the Research Grants from the Japan Prize Foundation, the Iketani Science and Technology Foundation, and the Research Encouragement Grants and the Continuation Grants for Young Researchers from the Asahi Glass Foundation (to YT). P. D. acknowledges the Polish National Science Centre funding, grant no. 2018/31/B/ST5/03085. YT and PD acknowledge the EU's Horizon 2020 for funding the OCTA project under grant agreement no. 778158.

Notes and references

1 M. Winkler and K. N. Houk, *J. Am. Chem. Soc.*, 2007, **129**, 1805–1815.
2 K. E. Maly, *Cryst. Growth Des.*, 2011, **11**, 5628–5633.
3 M. Etinski, J. Tatchen and C. M. Marian, *Phys. Chem. Chem. Phys.*, 2014, **16**, 4740–4751.
4 For selected reviews on purely organic TADF materials, see: (*a*) Y. Tao, K. Yuan, T. Chen, P. Xu, H. Li, R. Chen, C. Zheng, L. Zhang and W. Huang, *Adv. Mater.*, 2014, **26**, 7931–7958; (*b*) F. B. Dias, T. J. Penfold and A. P. Monkman, *Methods Appl. Fluoresc.*, 2017, **5**, 012001; (*c*) Z. Yang, Z. Mao, Z. Xie, Y. Zhang, S. Liu, J. Zhao, J. Xu, Z. Chi and M. P. Aldred, *Chem. Soc. Rev.*, 2017, **46**, 915–1016; (*d*) M. Y. Wong and E. Zysman-Colman, *Adv. Mater.*, 2017, **29**, 1605444; (*e*) M. Sarma and K.-T. Wong, *ACS Appl. Mater. Interfaces*, 2018, **10**, 19279–19304; (*f*) X. K. Chen, D. Kim and J.-L. Brédas, *Acc. Chem. Res.*, 2018, **51**, 2215–2224; (*g*) Y. Liu, C. Li, Z. Ren, X. Yan and M. R. Bryce, *Nat. Rev. Mater.*, 2018, **3**, 18020.
5 For selected reviews on purely organic RTP materials, see: (*a*) S. Mukherjee and P. Thilagar, *Chem. Commun.*, 2015, **51**, 10988–11003; (*b*) A. Forni, E. Lucenti, C. Botta and E. Cariati, *J. Mater. Chem. C*, 2018, **6**, 4603–4626; (*c*) H. Ma, A. Lv, L. Fu, S. Wang, Z. An, H. Shi and W. Huang, *Ann. Phys.*, 2019, **531**, 1800482; (*d*) Kenry, C. Chen and B. Liu, *Nat. Commun.*, 2019, **10**, 2111.
6 For selected reviews on azaacenes-based organic functional materials, see: (*a*) Q. Miao, *Synlett*, 2012, 326–336; (*b*) U. H. F. Bunz, J. U. Engelhart, B. D. Lindner and M. Schaffroth, *Angew. Chem., Int. Ed.*, 2013, **52**, 3810–3921; (*c*) J. Li and Q. Zhang, *ACS Appl. Mater. Interfaces*, 2015, **7**, 28049–28062; (*d*) U. H. F. Bunz and J. Freudenberg, *Acc. Chem. Res.*, 2019, **52**, 1575–1587.
7 For selected books and reviews on helical azaacenes, see: (*a*) I. Stary and I. G. Stará, in *Targets in Heterocyclic Systems*, ed. O. A. Attanasi, P. Merino and D. Spinelli, Italian Society of Chemistry, Roma, 2017, vol. 21, ch. 2, pp. 23–53; (*b*) K. Dhbaibi, L. Favereau and J. Crassous, *Chem. Rev.*, 2019, **119**, 8846–8953.

8 A. Klimash, P. Pander, W. T. Klooster, S. J. Coles, P. Data, F. B. Dias and P. Skabara, *J. Mater. Chem. C*, 2018, **6**, 10557–10568.
9 For a review on oxidative fusion and annulations of aromatic amines for the construction of π-conjugated organic compounds, see: S. Hiroto, *Chem. – Asian J.*, 2019, **14**, 2514–2523.
10 W. H. Perkin, *J. Chem. Soc.*, 1896, **69**, 596–637.
11 For a review on multi-photofunctional organic materials, see: P. Data and Y. Takeda, *Chem. – Asian J.*, 2019, **14**, 1613–1636.
12 Y. Takeda, M. Okazaki and S. Minakata, *Chem. Commun.*, 2014, **50**, 10291–10294.
13 P. E. Burrows, Z. Shen, V. Bulovic, D. M. McCarty, S. R. Forrest, J. A. Cronin and M. E. Thompson, *J. Appl. Phys.*, 1996, **79**, 7991–8006.
14 M. Okazaki, K. Takahashi, Y. Takeda and S. Minakata, *Heterocycles*, 2016, **93**, 770–782.
15 Y. Takeda, M. Okazaki, Y. Maruoka and S. Minakata, *Beilstein J. Org. Chem.*, 2015, **11**, 9–15.
16 For selected reviews on AIE and AIEE, see: (*a*) Y. Hong, J. W. Y. Lam and B. Z. Tang, *Chem. Soc. Rev.*, 2011, **40**, 5361–5388; (*b*) J. Mei, N. L. C. Leung, R. T. K. Kwok, J. W. Y. Lam and B. Z. Tang, *Chem. Rev.*, 2015, **115**, 11718–11940; (*c*) Y. Chen, J. W. Y. Lam, R. T. K. Kwok, B. Liu and B. Z. Tang, *Mater. Horiz.*, 2019, **6**, 428–433.
17 Y. Min, C. Dou, D. Liu, H. Dong and J. Liu, *J. Am. Chem. Soc.*, 2019, **141**, 17015–17021.
18 Y. Takeda, S. Ueta and S. Minakata, *Heterocycles*, 2017, **95**, 137–144.
19 M. A. El-Sayde, *Acc. Chem. Res.*, 1968, **1**, 8–16.
20 (*a*) Z. R. Grabowski and K. Rotkiewicz, *Chem. Rev.*, 2003, **103**, 3899–4031; (*b*) S. Sasaki, G. P. C. Drummen and G.-I. Konishi, *J. Mater. Chem. C*, 2016, **4**, 2731–2743.
21 P. Data, P. Pander, M. Okazaki, Y. Takeda, S. Minakata and A. P. Monkman, *Angew. Chem., Int. Ed.*, 2016, **55**, 5739–5744.
22 J. Li, T. Nakagawa, J. MacDonald, Q. Zhang, H. Nomura, H. Miyazaki and C. Adachi, *Adv. Mater.*, 2013, **25**, 3319–3323.
23 For selected reviews on orange-to-NIR emitters, see: (*a*) C.-T. Chen, *Chem. Mater.*, 2004, **16**, 4389–4400; (*b*) G. Qian and Z. Y. Wang, *Chem. – Asian J.*, 2010, **5**, 1006–1029.
24 M. Okazaki, Y. Takeda, P. Data, P. Pander, H. Higginbotham, A. P. Monkman and S. Minakata, *Chem. Sci.*, 2017, **8**, 2677–2686.
25 For a review on solvatochromic probes, see: A. S. Klymchenko, *Acc. Chem. Res.*, 2017, **50**, 366–375.
26 D. de Sa Pereira, P. L. dos Santos, J. Ward, P. Data, M. Okazaki, Y. Takeda, S. Minakata, M. Bryce and A. P. Monkman, *Sci. Rep.*, 2017, **7**, 6234.
27 K. Sun, Z. Cai, J. Jiang, W. Tian, W. Guo, J. Shao, W. Jiang and Y. Sun, *Dyes Pigm.*, 2020, **173**, 107957.
28 (*a*) G. Wei, L. Ying, D. Wenpeng, Z. Lei, N. Jinghua, L. Xia and A. Ping, *Chi. Pat.*, CN110240594A, 2019; (*b*) G. Wei, L. Ying, Z. Lei, D. Wenpeng, N. Jinghua and H. Gaojun, *Chi. Pat.*, CN110156663A, 2019.
29 For selected reviews on MCL materials, see: (*a*) Y. Sagara and T. Kato, *Nat. Chem.*, 2009, **1**, 605–610; (*b*) A. Pucci, R. Bizzarri and G. Ruggeri, *Soft Matter*, 2011, **7**, 3689–3700; (*c*) Z. Chi, X. Zhang, B. XU, X. Zhou, C. Ma, Y. Zhang, S. Liu and J. Xu, *Chem. Soc. Rev.*, 2012, **41**, 3878–3896; (*d*) Z. Ma, Z. Wang, M. Geng, Z. Xu and X. Jia, *ChemPhysChem*, 2015, **16**, 1811–1828; (*e*) Y. Sagara, S. Yamane, M. Mitani, C. Weder and T. Kato, *Adv. Mater.*, 2016, **28**, 1073–1095; (*f*) S. Xue, X. Qiu, Q. Sun and W. Yang, *J. Mater. Chem. C*, 2016, **4**, 1568–1578; (*g*) P. Xue, J. Ding, P. Wang and R. Lu, *J. Mater. Chem. C*, 2016, **4**, 6688–6706; (*h*) C. Wang and Z. Li, *Mater. Chem. Front.*, 2017, **1**, 2174–2194.
30 (*a*) J. Daub, R. Engl, J. Kurzawa, S. E. Miller, S. Schneider, A. Stockmann and M. R. Wasielewski, *J. Phys. Chem. A*, 2001, **105**, 5655–5665; (*b*) A. Stockmann, J. Kurzawa, N. Fritz, N. Acar, S. Schneider, J. Daub, R. Engl and T. Clark, *J. Phys. Chem. A*, 2002, **106**, 7958–7970; (*c*) N. Acar, J. Kurzawa, N. Fritz, A. Stockmann, C. Roman, S. Schneider and T. Clark, *J. Phys. Chem. A*, 2003, **107**, 9530–9541; (*d*) H. Tanaka, K. Shizu, H. Nakanotani and C. Adachi, *J. Phys. Chem. C*, 2014, **118**, 15985–15994.
31 P. Data, M. Okazaki, S. Minakata and Y. Takeda, *J. Mater. Chem. C*, 2019, **7**, 6616–6621.
32 Y. Takeda, H. Mizuno, Y. Okada, M. Okazaki, S. Minakata, T. Penfold and G. Fukuhara, *ChemPhotoChem*, 2019, **3**, 1203–1211.
33 Y. Takeda, T. Kaihara, M. Okazaki, H. Higginbotham, P. Data, N. Tohnai and S. Minakata, *Chem. Commun.*, 2018, **54**, 6847–6850.
34 S. Izumi, H. F. Higginbotham, A. Nyga, P. Stachelek, N. Tohnai, P. de Silava, P. Data, Y. Takeda and S. Minakata, *J. Am. Chem. Soc.*, 2020, **142**, 1482–1491.